Capillary Transition Zones from a Core Analysis Perspective

Johne Alex Larsen, Trond Thorsen and Geir Haaskjold
Norsk Hydro Research Centre, N-5020 Bergen, Norway
E-mail: Johne.Alex.Larsen@hydro.com

Abstract

The capillary transition zone in a reservoir containing oil and water is located between the oil-water contact and the level where irreducible water is present. In low permeability reservoirs or in situations where the oil and water densities are similar, the transition zone can be extended to cover a vertical distance up to around a hundred meters As the water saturation varies with the vertical distance in the transition zone, relative permeabilities and the capillary pressure must be determined by incorporating hysteresis in the flow functions. Special care should be taken in performing core-flow experiments in order to obtain relevant flow functions at different positions in the transition zone. Generally, both relative permeabilities and capillary pressure becomes a function of the connate water saturation in the transition zone. The amount of mobile oil should be found in the general case by a correlation between initial oil saturation and residual oil saturation.

This paper will focus on experimental data, showing the impact of a water injection in an oil-water transition zone. The transition zone is obtained by gravity drainage of water by oil in an one metre, vertically oriented Berea composite core. An imbibition process is performed by injecting water from the bottom of the core. During this gravity stable water injection, the water front is (dynamically) monitored by X-ray *in-situ* saturation measurements. The remaining oil saturation after water injection is found as a function of height at various positions in the core and correlated to the initial oil saturation at the start of water injection. The novel data confirms a *Land*-type correlation between initial and remaining oil saturation. However, a high recovery, that cannot be predicted by the *Land* correlation, is observed for very low initial oil saturations. It is also found that the correlation between initial oil saturation and remaining oil saturation is dependent on the permeability in water-wet Berea. The dynamical *in-situ* saturation measurements are reproduced by numerical modelling incorporating *Killough* hysteresis in the oil relative permeability and capillary pressure functions.

Introduction

A capillary transition zone may be defined as the mixing zone that occurs between two phases due to the capillary pressure generated when the fluids are immiscible. The oil-water transition zone is constrained upwards by the oil zone where the water saturation is close or equal to the irreducible water saturation and constrained downwards by the *oil-water contact* (*OWC*). In practice as well as theory, it can be difficult to define the level where the transition zone enters the oil zone, since the capillary pressure versus saturation (Pc-S) function is asymptotic towards the irreducible water saturation. One possible way to limit the upward extent of the transition zone would be to make a restriction on the derivative of S with height: $\partial S/\partial z \leq \varepsilon$, where ε must be defined *a priori*. The bottom of the transition zone is often easier to define due to the interrelation with the *OWC*, however, the OWC may be diffuse and positioned with an uncertainty of several meters from the petrophysical interpretations. Usually, the oil water contact is defined using the *free water leve*l (*FWL* $\Leftrightarrow$ level where Pc=0) as the intersections of P_w (versus depth) measured in the water zone and P_o measured in the oil zone. The standard interpretation for a water-wet reservoir implies that the *OWC* will be above the *FWL* by a distance that is proportional to the entry pressure on the Pc-S curve[1]. The same proportionality will exist for oil-wet reservoirs, however, the *OWC* will be below the *FWL*. For reservoirs of mixed wettability and/or where the distribution of fluids in the transition zone is due to other processes than primary drainage, the position of the *OWC* in accordance with a given *FWL* seems to be less well understood.

The capillary transition zone may be divided into three different types, characterised by increasing order of geological complexity. The *homogenous* transition zone can be described by a single capillary pressure curve measured for either a drainage process or an imbibition process. The connate water saturation is increasing uniformly with increasing height above the *OWC*. The *layer-dependent* transition zone is characterised by thin low permeability layers within a high permeability environment. In this case the connate water saturation is dependent on the local permeability and porosity but it is rather uniform within a layer with approximately constant permeability and porosity. The *heterogeneous* transition zone is very complex and may contain a transition zone within each layer of constant porosity and permeability. Each layer will be assumed to be in capillary equilibrium and the connate water distribution in the reservoir must be found from a capillary pressure (or J-function) for each layer. In addition to the geological heterogeneity caused by variation in pore-size distributions with position in the reservoir, several other aspects might effect the complexity. One of these sources can be the assumption of equilibrium between gravity and capillary forces within the reservoir. Another, that the accumulation of the reservoir is or has been controlled by equilibrium between gravity and capillary forces. Neither of these assumptions may be correct, but from experience one may conclude that for many practical situations the accuracy of these assumptions are within reasonable margins. The equilibrium assumption gives the connate water distribution implicitly from equation 1

$$\Delta\rho g z = P_c\,, \tag{1}$$

where z is the vertical distance above *FWL* and $\Delta\rho$ is the density difference. This work is aimed to increase the understanding of vertical flow in a capillary transition zone with permeability contrasts by showing experimental results. It is assumed that the initial fluid distribution is generated as a primary drainage process and the experiment is carefully designed such that there are no changes in saturation direction during the establishment of the transition zone.

1. Process dependent fluid distribution in the reservoir

The connate water distribution in a reservoir is a product of the accumulation history and the chemical, biological and geological processes during thousands of years. Due to the slow progress of these processes there is a possibility that the connate water saturation distribution, even in mature reservoirs, still is changing. The mobility of water in the oil zone is very low and the connate water is mainly found as meniscus in small pore throats and in nooks and crannies[3]. The meniscus may be in hydrodynamic contact through thin films or they become trapped by precipitation of oil components on the pore walls. In this case the wettability has changed from a water-wet and initially water filled system to a more oil-wet system where the water saturation is irreducible. If the water menisci are in hydrodynamic contact down to low water saturations, a gravity drainage of water from the oil zone may continue at ultra low rates. This ultra low gravity drainage led *Muskat*[4] to believe that the connate water distribution found in oil reservoirs is a mixture of primary drainage and imbibition processes. The basic picture is that during and/or after the accumulation period, the water will drain from the upper part of the oil zone, which implies imbibition in the lower part of the oil zone or in the transition zone.

Leverett[5] had postulated, a couple of years earlier, that the connate water distribution should be found from the imbibition process, but as *Muskat* pointed out, it seems like *Leverett* never gave any clear arguments for his opinion. The general view that oil is transported through thin carrier beds and accumulated in a geological trap by draining the water downwards[6], implies that the connate

water is distributed according to the primary drainage process. This is the most common assumption used today although the accumulation phenomenon still seems to be uncertain from a research perspective. It is also often assumed that the connate water distribution in a reservoir is consistent with a strongly water-wet system, even though the flow behaviour indicates a more intermediate to oil-wet system[7]. The reason for this is that the alteration of wettability that occurs from adsorption of organic compounds of the oil do not alter the porespace distribution of oil and water significantly. Oil adsorbes on the pore wall where only thin molecular films of water are present. The connate water saturation is mainly located in the water menisci, which remain undisturbed in the small pore throats and in nooks and crannies.

For the oil-water transition zone, the connate water saturation increases and some of the pore bodies are filled with water. Close to the *OWC*, even the largest pores are filled with water and the water must be considered to have a high relative permeability. The wettability of the transition zone is often found to be water-wet and the water-wetness increases towards the *OWC*[8]. Thus, the connate water distribution from the *OWC* to the top of the reservoir is consistent with a strongly water-wet behaviour. However, if there is a concentration gradient in the oil with more heavy components in the lower part of the transition zone, the opposite wettability trend may occur. In this case a slight increase in oil-wet behaviour is seen in the transition zone compared to the oil zone and a possible lack of agreement may be seen between the capillary pressure characteristic of water-wet cores and the connate water distribution in the reservoir.

If the oil column is thick, a slow drainage of water from the upper part of the oil zone will give an imbibition distribution in most of the transition zone. When the imbibition has taken place in a pre-historic transition zone based on a primary drainage distribution, hysteresis must be emphasised in Pc-S in order to describe the present connate water saturation[2]. Generally, the new connate water distribution is found by using the imbibition Pc-S whenever the imbibition has occurred outside a historic transition zone. Several geological events can give the imbibition connate water distribution as described above. Among these can be rotation of the reservoir, leakage of hydrocarbons through the geological trap and pressure variations in the reservoir.

2. Fluid flow behaviour in the capillary transition zone

Numerical modelling of capillary transition zones is described in detail in reference 2, and only a brief discussion will be given here. During secondary migration, oil accumulates in geological traps and displaces water downwards[6] as shown in Figure 1a. Since most reservoirs are initially considered 100% water filled and water-wet, this process is similar to primary drainage. Thus, the connate water distribution above the FWL will be determined by the capillary pressure curve for primary drainage. The connate water distribution is defined to be the water saturation which is present in the reservoir at the time of discovery and therefore prior to any production. Subsequent upward movement of the FWL, either in geological time or during production will change the distribution in the transition zone from a primary drainage condition to an imbibition condition. For the discussion in this paper as well as the reported experimental study, primary drainage condition is assumed initially everywhere in the reservoir.

In Figure 1a an arbitrary point (A) located in the capillary transition zone has historically been drained from 100 % water saturation to a connate water saturation that is higher than the irreducible water saturation. The "hold-up" of water indicated by the stable situation in Figure 1a is due to capillarity but even though this is a stable situation both oil and water must be considered to be mobile in the transition zone (finite relative permeabilities). The relative permeabilities and

capillary pressure are given schematically in Figure 1b for both the accumulation process and during production with water influx into the transition and oil zones. Imbibition scanning curves from the connate water saturation to the residual oil saturation (ROS) describe the flow in the transition zone. Note that the endpoints of the scanning-curves have not been included in Figure 1b and only the general hysteresis trends have been sketched. For the completely water-wet case, minor hysteresis is expected in the water relative permeability[16] and there is no negative capillary pressure for water saturations higher than (1-S_{or}). Several algorithms for calculating scanning curves have been published in the past and some frequently cited are found in references 9,10,11 and 12. Many researchers have reported a relationship between ROS and the historical maximum oil saturation (HMOS) on the core scale[8,12,15] and it must be assumed for the general case that ROS is lower in the transition zone than in the oil zone. The major difficulty with hysteresis related to the transition zone is the possible variation of wettability with connate water saturation. If present, this should be accounted for both in SCAL studies and by defining appropriate rock types in the numerical model.

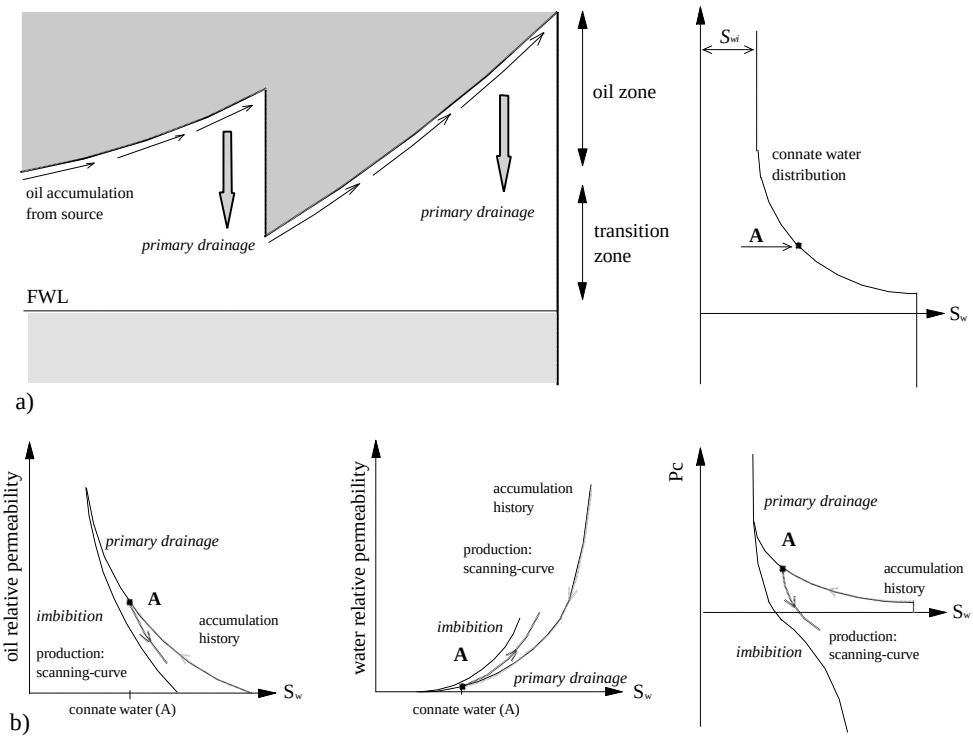

Figure 1. Schematic illustration of secondary migration and oil accumulation in geological traps **(a)**. Gravity drainage of water by oil gives a connate water distribution based on the primary drainage capillary pressure. In the transition zone, water influx during production must be described by imbibition scanning-curves for both relative permeabilities and capillary pressure **(b)**

Knowledge of the residual oil saturation in the transition zone is especially important when a significant amount of the total oil reserve is located in areas with high connate water saturation. It is usual to consider the ROS to be dependent on the HMOS based on single-core experiments. Several publications[13,14,15] have reported results where the initial non-wetting saturation (gas or oil) has been varied prior to the imbibition. In such experiments an uniform initial saturation is obtained by the steady-state technique[13], membranes[14] or evaporation[15] (gas-oil). When the core is flooded

with water, a relationship between the initial oil saturation and the ROS can be found by repeated experimentation with different initial saturations. In strongly wetted systems, the results of such experiments leads to a Land-type[15] relationship between *HMOS* and *ROS* as given in equation 2

$$ROS = \frac{HMOS}{1 + C \cdot HMOS}, \qquad (2)$$

where *C* is a constant dependent on the pore-size distribution function and wettability. For systems of mixed or intermediate wettability, however, several authors[8,13] have reported other functional relationships than the usual Land-type. If the ROS is not uniformly increasing with increasing HMOS, as assumed in Eq. 2, some of the imbibition scanning-curves for relative permeabilities and capillary pressure must intersect. *In-situ* saturation monitoring should be used in experiments where ROS are determined as function of HMOS. Local imbibition effects during the experiment may alter the pore distribution of oil and water compared to the primary drainage distribution assumed for the transition zone. This will probably be most critical at low oil saturations where water has a high relative permeability[18]. The main purpose of the experiment reported in this paper is to overcome the uncertainty of the HMOS distribution by designing an experiment similar to the accumulation of oil in the reservoir. Secondly, *in-situ* saturation measurements are used to establish the relationship between ROS and HMOS. These data will not describe the transition zone if the fluid distribution is generated by imbibition.

3. Experimental set-up

The gravity drainage part of the experiment is illustrated in Figure 2**.** It is a closed system where oil is replaced at the top of the core as water is drained out at the bottom. For the succeeding water injection, a differential pressure system was installed across the core, and the outlet at the top of the core was led through a back-pressure regulator at 20 bar. **A synthetic fluid system** was used for this experiment. Composition of the synthetic seawater (SSW) is listed in Table 3.1. NaI was added to the SSW to cover a wider capillary pressure curve in the one metre core, as the capillary pressure is directly dependent on the density difference (Eq. 1). The amount of NaI added was determined from experimental design using a laboratory simulator. These simulations gave an optimum density difference of the given system. 842 g NaI was added to 1000 ml SSW, giving a water(SSW+NaI) density of 1.53 g/cm^3. The water was filtered using a 0.45 μm filter prior to injection. n-decan with a density of 0.73 g/cm^3 was used as the oil phase.

Table 3.1. Synthetic seawater compositions

Salt	Content [g/l]
NaCl	24.89
$CaCl_2\,2H_20$	1.726
$MgCl_2\,6H_20$	11.124
$NaHCOl_3$	0.192
Na_2SO_4	4.056
KCl	0.668

The rock sample used was a composite Berea outcrop core. Individual core-element properties are listed in Table 3.2. The composite core was assembled with the following core order from top: 1-2-3-4-5. The total length of composite core was 95.1 cm, with a pore volume of 221.4 ml.
Permeability of the composite core was measured as 340 mD (100% water saturated).

Table 3.2. Core properties

Core ID	Length [cm]	Diameter [cm]	Porosity	Permeability n-Decan [mD]
#1	29.3	3.72	0.225	740
#2	18.2	3.72	0.179	120
#3	22.5	3.72	0.223	670
#4	22.4	3.72	0.224	716
#5	2.8	3.72	0.179	70

In-situ saturation measurements were done using an X-ray system consisting of a Kevex PXS5-701SA X-ray source (70 kV, 0.1 mA) and a detector system with a NaI scintillation detector with photo-multiplier and multi-channel analyser. The detector is collimated with a 5-mm slit opening perpendicular to the core axis. A gross count is measured at every centimetre along the core. Thus, an average saturation is calculated for every one centimetre slice along the core. During the experiment, source voltage was 52 kV and source current 0.05 mA. In-situ saturation profiles were calculated using the following formula:

$$S_o = \frac{\ln I - \ln I_w}{\ln I_o - \ln I_w}, \qquad (3)$$

where S_o : oil saturation, I: intensity (gross counts) at current saturation, I_w : intensity at 100% water saturation and I_o : intensity at 100% oil saturation. The uncertainties of the oil saturation measurements is in the order of 0.01-0.02 (saturation fractions) and the I_w was 1900 counts and I_o 34300 counts.

4. Results and discussion

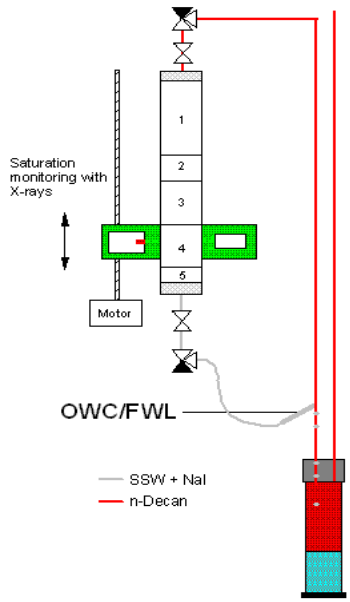

The primary drainage saturation distribution was obtained by free gravity drainage of water by oil from the top of the vertical core. The position of the FWL was established using the experimental set-up as shown in Figure 2. The depth of FWL relative to the core was set to allow oil to enter the low permeability core #2, but not the low permeability core#5. The capillary entry-pressure for the low permeability cores was measured to be about 50 mbar.

The gravity drainage process was kept under surveillance by in-situ saturation measurements every second hour. Even though the position of the FWL gave a capillary entry-pressure at the bottom of core#2 that was about 20-30 % higher than the measured value, it turned out that the free gravity drainage process progressed too slowly in the low permeability core. Therefore, a forced gravity drainage was started by injecting oil from the top at ultra-low rates (0.002-0.004 ml/min) and continued until the oil saturation started to increase in core#3.

Figure 2. Experimental set-up

After the forced gravity drainage the system was again set to free gravity drainage and the final primary drainage (P.D.) connate water distribution was obtained as seen in Figure 3. During the free and forced gravity drainage processes, no saturation reversals (imbibition) were observed from primary drainage, except from in the vicinity of the joining region between the high permeability core #1 and the low permeability core#2. In this area imbibition was recognised, but the saturation changes were at maximum only 0.02 fraction units. The final transition zone was established when the saturation profile was found to be stable within the measurement uncertainty during a two week period. The total time spent in order to establish the transition zone was two and a half month.

The saturation profiles from the low rate (0.012 ml/min) water injection are shown in Figure 3. Oil was found to accumulate in the joining region between the high permeability cores (core#4 & core#3). This oil accumulation is probably due to capillary effects either caused by small cavities in the joining, higher local permeability, or lack of capillary continuity over all the joining area. In the high permeability core#3, a capillary end-effect was observed towards the low permeability core. A conventional end-effect is observed at the outlet. The ultra low rate was increased after about 0.3 PV of water injection to 0.35 ml/min and after 5 PV to 3.5 ml/min. A minor decrease in oil saturation in response to increased water injection rate can be observed away from the areas affected by capillary connection effects and capillary end-effects. A major decrease in the oil saturation is achieved in the areas influenced by the capillary effects as seen in Figure 3. The measured oil production after the increase in flow rate was about 1.5 ml.

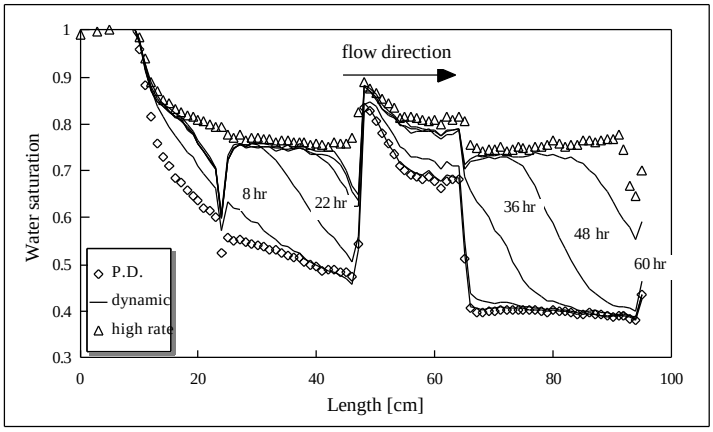

Figure 3. In-situ water saturation profiles. The initial primary drainage distribution is shown together with the dynamical profiles after 8, 22, 36, 48 and 60 hours of ultra-low rate waterflood. The final profile after high rate waterflood is also shown.

The relationship between ROS and HMOS is given in Figure 4a when the ROSs are equal to the local saturation after *i*) the ulta-low rate water flood and *ii*) the high rate water flood. Data are given for both the low permeability (~100 mD) Berea and the high permeability (~700mD) Berea. The scatter in the datapoints is mostly found to be caused by the capillary affected areas. The Land relation is plotted in Figure 4a with Land constants equal to 1, 2 and 5. A Land constant of 5 is used to give the ROS from low HMOS and a Land constant of about 2 is appropriate for the higher HMOS. The Land relation with a single constant will predict too low values of ROS at high HMOS and too high values of ROS at low HMOS.

The oil recovery after high flow rate is given in Figure 4b as a function of the HMOS. Only datapoints outside the capillary affected areas are used. It is apparent that the recovery from the low permeability Berea is lower than the high permeability Berea. Before simulation of the experiment, it was uncertain whether this observation is caused by different ROS vs HMOS relationships for

high and low permeability Berea or the observation is caused by a longer time needed to waterflood the low permeability core to ROS. The oil recovery from the high permeability core is about 58 % from 0.6 HMOS to about 45 % at 0.2 HMOS. The low permeability core has a narrower HMOS interval, but confirm the trend with lower recovery at lower HMOS. Data from Davis[13] *et. al*. and Pickell[14] *et. al*. are also shown in Figure 4b and confirms the trend in the data reported in this study. They used a steady-state technique (Davis) and membrane (Pickell) and observed lower recovery for low HMOS than this present work.

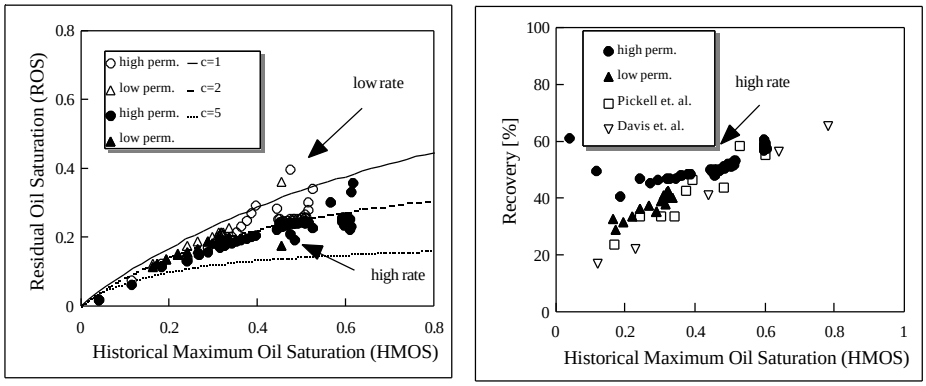

a) b)

Figure 4. ROS and oil recovery as function of HMOS. **(a)** The residual oil saturation is plotted as function of the historical maximum oil saturation along the core. Scatter in the data is due to capillary effects at the joining region between core elements and the capillary end-effect. The Land relation is shown with Land constants of 1, 2 and 5. **(b)** The oil recovery is calculated as percent of the HMOS remaining after the high rate waterflood. Also shown is data from Davis[13] and Pickell[14].

The simulation model for the transition zone experiment utilised Killough[10] hysteresis in both oil relative permeability and capillary pressure while the water relative permeability was assumed to be independent of process. It is well documented that the hysteresis in the wetting phase relative permeability is negligible[16] or small[19-23] for strongly wetting systems. The simulation approach follows the principles in Figure 1b with the connate water distribution as shown by the primary drainage profile in Figure 3. Input data to the hysteresis model was generated in the following manner: Primary drainage relative permeabilities for core#1 and core#2 were found from a separate unsteady-state experiment. The results are given in Figure 5. These two cores are assumed to be representative for the high permeability regions (core#1,#3,#4) and the low permeability regions (core#2,#5) of the composite core, respectively. Both an analytical approach[17] and a parameter estimation technique were used to find the relative permeabilities. For this particular case, there was only a minor difference in the results from these two methods. The imbibition relative permeability for water was set to be equal to the primary drainage curve. The imbibition relative permeability to oil was found from the primary drainage curve by an algorithm of Carlson[9] using a Land constant of 2 for the low permeability cores and 3 for the high permeability cores. The value of the Land constant was found from the experimental data in Figure 4a. The water relative permeability and the oil relative permeability bounding curves are given in Figure 5a for the low permeability core and in Figure 5b for the high permeability core. The simulations confirmed that the Land constant is dependent on permeability in Berea sandstone. One single constant independent of permeability was found to give a poor match to the *in-situ* saturation profiles.

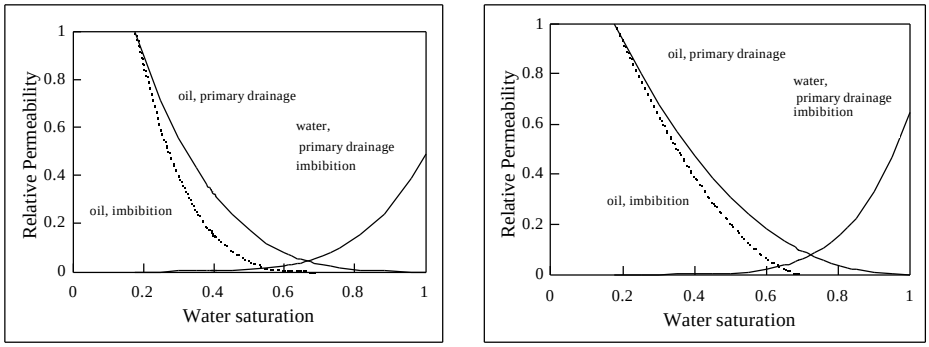

Figure 5. Water and oil relative permeabilities**.** High permeability (700 mD) Berea core **(a)** and low permeability (100 mD) Berea core **(b)**. The primary drainage (PD) relative permeabilities are measured by unsteady-state experiments. No hysteresis is expected in the water relative permeability.

The capillary pressure for primary drainage was calculated from the initial saturation profile assuming equilibrium between capillary forces and gravity (Eq. 1). The primary drainage Pc was used to initialise the connate water in the simulation model. The result is shown in Figure 6a.

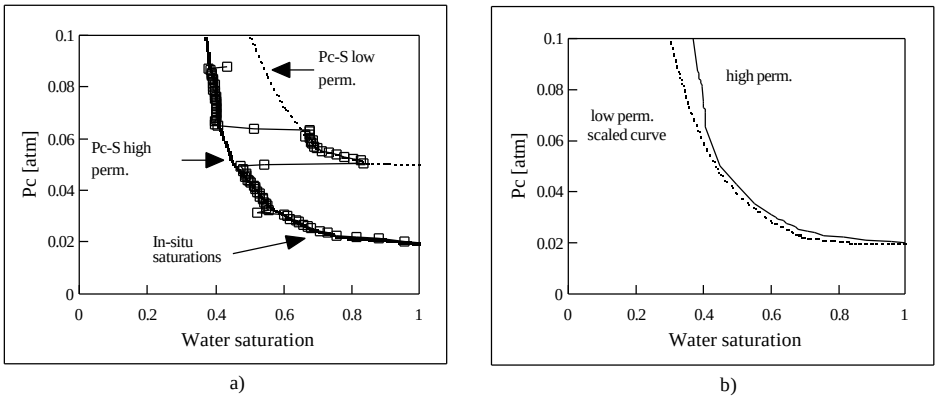

Figure 6. Equilibrium calculations of Pc-S from *in-situ* saturation measurements**.** The capillary pressure as function of saturation is calculated by knowing the height above FWL and assuming equilibrium between gravity and capillary forces **(a)**. The low permeability capillary pressure curve is scaled with permeability and porosity to the analogue values of the high permeability curves (J-function approach). Agreement between the capillary pressure for low and high permeability Berea is obtained **(b)**.

The capillary entry pressure of the low permeability core estimated by calculating the height above the FWL was consistent with the measured value (50 mbar). The Pc-S curves for the low and high permeability cores could be scaled by permeability and porosity to the same curve as shown in Figure 6b. Capillary pressure for imbibition was included in the simulations (Killough hysteresis) and estimated by using an expression by *Skjæveland*[12] where the parameters have been tuned until the curve fit Pc=0 at the residual oil saturation. The simulated water saturation profiles are shown together with the measured profiles for the ultra-low rate water flood in Figure 7.

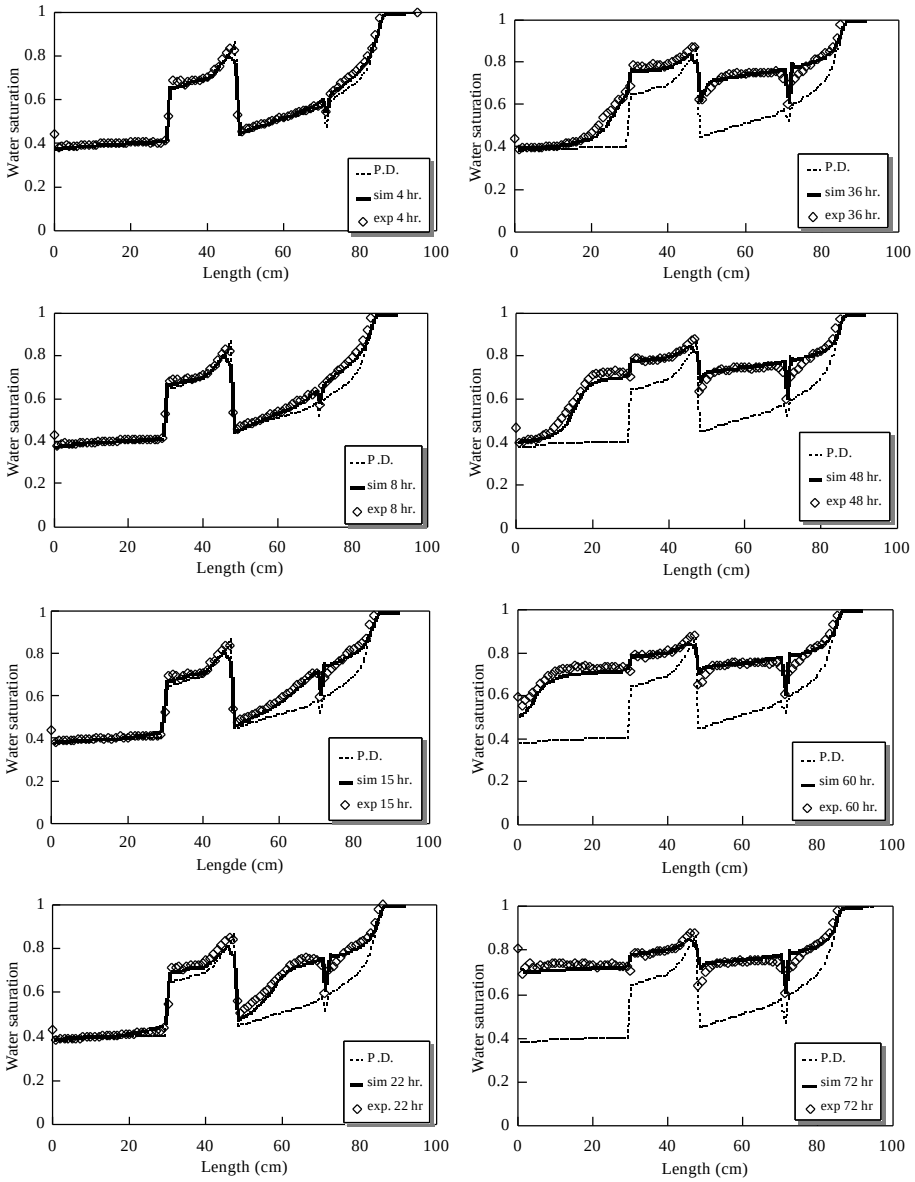

Figure 7. Simulated and experimental in-situ saturation profiles.

The simulated profiles were predicted using the input as described above and were not obtained from any history matching procedure. The only exception is that the imbibition capillary pressure was adjusted in one local gridblock at the joining between core#3 and core#4. The adjustment was necessary in order to describe the oil accumulation at the joining of the two cores. In general there is good agreement between the simulated profiles and the measured profiles. Some differences are observed in the areas that are effected by the capillary affects as described above; however, the use of hysteresis scanning curves in modelling the water influx into the transition zone is concluded to be essential. Simulations based on relative permeabilities with end-point scaling of the saturation interval[25] or imbibition bounding curves were found to give a poor match to the dynamic saturation profiles.

The experimental results obtained in this study should be compared against similar results from other authors[13-15] using different types of experimental approaches. For initial oil saturations above about 30 %, it seems like the ROS distribution is independent of the method used to establish the initial saturations. Below this value, the experiment used in this study seems to give lower ROS than the evaporation methods (trapped gas instead of ROS), steady-state methods or membrane techniques on single cores[13-15]; however, few data are published for such low initial non-wetting phase saturations. The same trend, but less distinctive, as reported in this work may be found in Land's original work[15] using the evaporation method in a gas-oil system where gas is the non-wetting phase. General conclusions are not possible due to different fluid systems, wettability and/or core material.

The reason for the possible discrepancy at low initial oil saturation is believed to depend on the pore-level distribution of wetting and non-wetting phase prior to the imbibition process. In this work the dynamic process that generates the primary drainage saturation profile is close to capillary equilibrium for all times and saturations. Thus, trapping of the non-wetting phase should be negligible for a strongly wetting system. The steady-state method used in repeated single core experiments with uniform saturation distribution[13] has been shown by Salter & Mohanty[18] to give trapping of non-wetting phase even for primary drainage. The trapping is most distinctive at low oil saturations and vanishes when the oil saturation is higher than about 30%, which supports the assumption that the pore level fluid distribution is dependent on method and force regimes. Further research should emphasise the possible problems caused by using steady-state experiments to determine ROS, but also relative permeabilities for the low oil saturation in the capillary transition zone.

5. Summary and Concluding remarks

The following should be considered in *special core analysis* relevant for the capillary (oil-water) transition zone:

i) The historical processes in the reservoir, which have generated the connate water distribution (primary drainage, imbibition, etc.).
ii) Wettability distribution (constant or dependent on connate water).

<u>If the connate water is distributed according to the primary drainage process, then:</u>

iii) Find the appropriate empirical relation between ROS and HMOS.
iv) HMOS is equal to the connate water saturation in the transition zone.
v) The flow of oil and water in the transition zone is described by imbibition scanning curves with origin at the connate water saturation on the respective primary drainage curves.
vi) Measure the bounding curves for each wettabillity regime and calculate the scanning-curves from an appropriate algorithm[10-12].

<u>If the connate water is distributed according to the imbibition process, then:</u>

vii) Set ROS equal to the residual oil saturation in the oil zone and not as a function of the connate water saturation in the transition zone.
viii) The oil-water flow in the transition zone is described by imbibition bounding curves for relative permeabilities and capillary pressure.

Based on the experimental work on water-wet Berea sandstone the following conclusions are valid:

1) Residual oil saturation is locally a function of the historical maximum oil saturation.
2) The residual oil saturation can be estimated from the maximum historical oil saturation using a Land relation; however, the Land relation seems to predict too high residual oil saturation for low historical maximum oil saturations.

3) The residual oil saturation as a function of the maximum historical oil saturation is found to be different for 700 mD Berea compared to 100 mD Berea.
4) Numerical simulations have proven the importance of using hysteresis scanning-curves in both relative permeabilities and capillary pressure to describe the flow in the transition zone.

References:

1. Desbrandes, R. and Gualdron, J.:"In Situ Rock Wettability Determination with Wireline Formation Tester Data", The Log Analyst (1988), July-August, P. 244-251.
2. Eigestad, G.T. and Larsen J.A.:"Numerical Modelling of the Capillary Transition Zone", SPE 64374, to be presented at the 2000 SPE Asia Pacific Oil & Gas Conference and Exhibition
3. Chapman, R.E.:"Effects of Oil and Gas Accumulation on Water Movement", *The American Association of Petroleum Geologists* (March 1982), **V 66**, No 3, P. 368-378.
4. Muskat, M.:"Calculation of Initial Fluid Distributions in Oil Reservoirs", *Petroleum Tech.*, Tech. Pub. No. 2405, (July 1948), P. 119-127.
5. Leverett, M. C.:"Capillary Behavior in Porous Soils", Trans AIME (1941), 142, P. 152-169.
6. Chapman, R.E.:"Petroleum Geology", Elsevier Scientific Pub. Co., 1983.
7. Swanson, B.F."Rationalizing the Influence of Crude Wetting on Reservoir Fluid Flow With Electrical Resistivity Behavior", *Journal of Petroleum Technology* (August 1980), P. 1459-1464.
8. Jerauld, G.R. and Rathmel, J. J."Wettability and Relative Permeability of Prudhoe Bay:A Case Study in Mixed-Wet Reservoirs", *SPE Reservoir Engineering* (Feb. 1997), P. 58-65.
9. Carlson, F. M.: "Simulation of Relative Permeability Hysteresis to the Nonwetting Phase, SPE 10157, presented at the 56th Annual Fall Tech. Conf. of the SPE-AIME, (1981),San Antonio, TX.
10. Killough, J. E.: "Reservoir Simulation with History-Dependent Saturation Functions," *SPEJ* (Feb. 1976), *Pet. Trans. AIME* **261**, 37-48.
11. Kjosavik, A., Ringen J.K and Skjæveland, S.M.:"Relative Permeability Correlations for Mixed-Wet Reservoirs", SPE 59314 presented at the 2000 SPE/DOE IOR Symp., Tulsa, 3-5 april.
12. Skjæveland, S.M., Siqveland, L.M., Kjosavik, A., Hammervold, W.L. and Virnovsky, G.A.:"Capillary Pressure Correlation for Mixed-Wet Reservoir", SPE Reservoir Eval. & Eng. (Feb. 2000), **3** (1), 60-67.
13. Davies, G.W. and Gamble, I.J.A.:"Field-Wide Variations in residual oil Saturations in a North Sea Sandstone Reservoir", SPE 19851 presented at the 64th ATCE, San Antonio, TX, October 8-11, 1989.
14. Pickell, J.J., Swanson, B.F. and Hickman, W.B.:"Application of Air-Mercury and Oil-Air Capillary Pressure Data in the Study of Pore Structure and Fluid Distribution", *SPEJ* (Mar. 1966), P. 55-61.
15. Land, C. S.: "Comparison of Calculated with Experimental Imbibition Relative Permeability," Soc. *Pet. Eng. J.* (Dec 1971) *Pet. Trans. AIME* 251, 419-425.
16. Braun, E.M. and Holland R.F.:"Relative Permeability Hysteresis: Laboratory Measurements and a Conceptual Mode, SPERE (Aug. 1995), P. 222-228.
17. Johnson, E.F., Bossler, D.P. and Naumann, V.O.:"Calculation of Relative Permeability from Displacement Experiments", *Pet. Trans. AIME* 210 (1959), 370-372.
18. Salter, S.J. and Mohanty, K.K."Multiphase Flow in Porous Media: I, Macroscopic Observations and Modeling.", SPE 11017 presented at the 57th ATCE, New Orleans, LA, Sept. 26-29, 1982.
19. Osoba, J. S., Richardson, J.G., Kerver, J. K., Hafford, J. A., and Blair, P. M.: " Laboratory Measurements of Relative Permeability" , *Pet. Trans. AIME* **191**, 47-56, 1951.
20. Geffen, T. M., Owens, W. W., Parrish D. R. and Morse, R. A.:" Experimental Investigation of Factors Affecting Laboratury Relative Permeability Measurements," *Pet. Trans. AIME* **191**, 99-110,1951.
21. Naar, J., Wygal, R. J. and Henderson, J. H.: "Imbibition Relative Permeability in Unconsolidated Porous Media," *SPEJ* **2**, 13-17, 1962.
22. Talash, A. W.: "Experimental and calculated Relative Permeability Data for Systems Containing Tension Additives," SPE#5810, presented at the Symposium on Improved Oil Recovery, Tulsa, OK, March 22-24, 1976.
23. Fulcher, R. A., Ertekin, T. and Stahl, C. D.: " The Effect of the Capillary Number and Its Constituents om Two-Phase Relative Permeability Curves," Paper SPE 12170, presented at the 58th Ann. Tech. Conf., San Fransisco, CA, (Oct., 5-8 1983)
24. Jerauld, G. R. and Salter, S. J.: "The Effect of Pore-Structure on Hysteresis in Relative Permeability and Capillary Pressure: Pore-Level Modeling," Transport in Porous Media Volume 5, 1990.
25. "Eclipse 100, Technical Appendices", 94a

Acknowledgement

The authors acknowledge Norsk Hydro for permission to publish this paper.